$KMg_{1-x}Pd_xF_3$ with perovskite-like structures as precursors for the catalytic hydroconversion of CCl_2F_2 and $CHClF_2$

A. Morato [a], C. Alonso [a], F. Medina [a,*], J.L. Garreta [a], J.E. Sueiras [a], Y. Cesteros [b], P. Salagre [b], D. Tichit [c] and B. Coq [c]

[a] *Departament d'Enginyeria Química, ETSEQ, Universitat Rovira i Virgili, Pl. Imperial Tarraco 1, 43005 Tarragona, Spain*
E-mail: fmedina@etse.urv.es
[b] *Facultat de Química, Universitat Rovira i Virgili, Pl. Imperial Tarraco 1, 43005 Tarragona, Spain*
[c] *Laboratoire de Matériaux Catalytiques et Catalyse en Chimie Organique, UMR CNRS-ENSCM 5618, 8 rue de l'Ecole Normale, 34296 Montpellier Cedex 5, France*

Received 5 June 2001; accepted 9 August 2001

Several fluoride type perovskites, with formula $KMg_{1-x}Pd_xF_3$, have been prepared for the first time. The enlargement of their cell parameters has been associated with the insertion of Pd into the structure. After reduction, these new compounds, when tested in the hydrodechlorination reaction of CCl_2F_2 and $CHClF_2$, showed higher selectivities to $CHClF_2$ and CH_2F_2, respectively, than other Pd catalysts supported on $KMgF_3$.

KEY WORDS: perovskite; CFC; palladium catalysts; hydrodechlorination

1. Introduction

Catalytic removal of chlorine from organic compounds such as chlorofluorocarbons (CFCs) and hydrochlorofluorocarbons (HCFCs) is of increasing interest on account of their high contribution to the depletion of the ozone layer [1–3]. The CFCs are being reduced owing to the United Nations Environmental Protection Protocol for CFC regulation adopted in Montreal, Canada, in 1987 and later meetings, which promulgated a set of guidelines to restrict the production of CFCs and eliminate the use of specific CFCs [4,5]. Moreover, the CFCs are being replaced at present by HCFCs as transition compounds in some kind of applications. For example, $CHClF_2$ (HCFC-22) is used as refrigerant in air conditioners.

However, HCFC compounds do not exhibit null values of ozone-depleting potential (ODP). Then, it is planned to replace in the near future all the CFCs and HCFCs by more environmental friendly products as HFCs, with very low or null ODP. Therefore, in the next years, the main stocks will be HCFCs, especially HCFC-22.

In order to eliminate these substances, many destruction techniques have been proposed [6–9] but it appears more interesting to convert CFCs and HCFCs into valuable chemical compounds such as HFCs. For this purpose, noble metals have been mainly used as catalysts for CFC hydrodechlorination. Palladium is the preferred active metal for this reaction, in particular, supported palladium is the most widely used catalyst [10–29]. The role of the support appears important for the development of new catalysts capable of very selective chlorine removal from CFC molecule because the metal–support interaction can modify favourably the electronic state of the metal particles [17,18]. Support effects from fluoride-based materials have been identified as a clue to achieve high selectivity to HFCs [12,16,18].

Perovskite-like structure materials have been of great interest to the condensed matter physics, solid-state chemistry and materials science communities over the past four decades [30]. Fluoride perovskites of $A^+B^{2+}F_3$ type form a large family of compounds, which show various interesting structures. These complex fluorides have been extensively studied due to their particular physical properties such as piezoelectric characteristics [31,32], photoluminescence behaviour [33], ionic conductivity [34] and nonmagnetic insulator behaviour [35]. Complex fluorides are usually prepared by solid-state reaction at high temperature [30,34,36–39]. Recently, the preparation of complex fluorides with perovskite-like structure, in solid-state reaction, has been reported at milder conditions (353–513 K) [40–42]. This synthesis route to complex fluorides can be a useful method for the obtention of micro-mesoporous solids with high surface areas. Besides, these materials may exhibit interesting acid–basic properties and the challenging introduction of some B^{2+} reducible noble metal cations in the structure can yield supported noble metal catalysts, after reduction. In these materials both the metallic function and the acid–basic properties might be tailored through several parameters such as nature and amount of the cations and activation conditions. On that account, these materials would be of special interest for hydrogenation reactions in which the catalytic properties could be modified by tuning the acid or basic sites of the support, *i.e.*, "electron acceptor or donor" properties.

* To whom correspondence should be addressed.

1011-372X/01/1100-0141$19.50/0

In this work, we have investigated the catalytic properties, after reduction, of $KMg_{1-x}Pd_xF_3$ with perovskite structures in the hydrodehalogenation reaction of CCl_2F_2 (CFC-12) and $CHClF_2$ (HCFC-22) in the gas phase. These perovskite structures have been prepared by the not yet reported hydrothermal synthesis method (at 333 K in aqueous medium). Also, one sample of pure $KMgF_3$ was impregnated with palladium in order to compare its catalytic behaviour with the results obtained by using the reduced $KMg_{1-x}Pd_xF_3$ samples.

2. Experimental

The hydrothermal synthesis of $KMg_{1-x}Pd_xF_3$ compounds with perovskite-like structures were performed as follows: a solution with appropriate amounts of $Mg(NO_3)_2 \cdot 6H_2O$ and $PdCl_2$ was precipitated with a solution of KOH (0.1 M) at room temperature and pH = 10. The obtained precipitate was filtered and washed with distilled water to eliminate KOH excess. The gel was then suspended at room temperature in a Teflon vessel in distilled water under magnetic stirring. An appropriate amount of two aqueous solutions of KOH and HF (both 0.1 M) was added dropwise until pH $\approx$ 6–7 was achieved. The mixture was then stirred and heated at 333 K for 12 h. The solid formed was filtered, washed with distilled water and ethanol and dried at 373 K overnight.

Three samples with K/Mg/Pd/F ratios of 1/1/0/3, 1/0.98/0.02/3 and 1/0.93/0.07/3 were synthesized by this method and labelled as S_1, S_2 and S_3, respectively. Another sample (called S_4) was prepared by impregnating the pure $KMgF_3$ with palladium in a similar amount as for the S_3 sample.

Samples S_2, S_3 and S_4 were reduced in a H_2/Ar flow (10/90 vol/vol) at 523 K for 4 h. These catalysts are labelled as S_{2R}, S_{3R} and S_{4R}, respectively.

The samples and catalysts were characterised by X-ray diffraction (XRD), N_2 adsorption (BET surface area), hydrogen chemisorption, thermogravimetric analysis (TGA), X-ray fluorescence, scanning electron microscopy (SEM) and infrared spectroscopy (FT-IR).

Powder X-ray diffraction patterns (XRD) of the samples were obtained with a Siemens D5000 diffractometer using a nickel-filtered Cu Kα radiation. Samples were dusted on double-sided sticky tape and mounted on glass microscope slides. The patterns were recorded over a range of 2θ angles from 7° to 70° and the crystalline phases were identified using the files of the Joint Committee on Powder Diffraction Standards (JCPDS). The JCPDS files used were 18-1033, 1-1107, 5-0681, 41-1443 and 75-0296 for the perovskite, PdO, Pd, MgF_2 and KCl phases, respectively.

The BET surface areas were calculated from the nitrogen adsorption isotherms at 77 K using a Micromeritics ASAP 2000 surface analyser and a value of 0.164 nm^2 for the cross-section area of the nitrogen molecule.

The hydrogen chemisorption was measured with a Micromeritics ASAP 2010C instrument equipped with a turbomolecular pump. Samples had previously been reduced in the same conditions in which the catalysts had been prepared. After reduction, the hydrogen on the nickel surface was removed with 30 ml min^{-1} of He for 30 min at 683 K. The sample was subsequently cooled to 303 K under the same He stream. The chemisorbed hydrogen was analysed at 343 K using the adsorption–backsorption isotherm method proposed by Benson *et al.* [43] to eliminate the contribution of β-PdH phase. The nickel surface atoms were calculated assuming a stoichiometry of one hydrogen molecule adsorbed per two surface nickel atoms and an atomic cross-sectional area of 6.49×10^{-20} m^2/Ni atom.

TGA analyses were carried out in a Perkin–Elmer TGA 7 microbalance equipped with a 273–1273 K programmable temperature furnace. Each sample (30 mg) was heated in a Ar flow (80 cm^3 min^{-1}) from 323 to 873 K at 10 K min^{-1}.

X-ray fluorescence analyses were made with a Philips EM 301 microscope equipped with an electron probe microanalyser (EPMA), CAMECA Camebax SX-50, and operating at acceleration voltages between 35 and 45 kV. The atomic ratios of F, K, Mg and Pd of the samples were obtained.

Scanning electron micrographs were obtained with a Jeol JSM-35C scanning microscope operating at an accelerating voltage of 35 kV, a work distance (wd) between 10 and 13 mm and magnification values in the range 25000–40000×.

The infrared spectra (FT-IR) were recorded with a Nicolet 5ZDX spectrometer in the 4000–400 cm^{-1} wavenumber range using pressed KBr pellets.

The reaction of CCl_2F_2 and $CHClF_2$ with hydrogen was carried out at atmospheric pressure in a microflow reactor (filled with 250 mg of catalyst) at 1000 h^{-1} space velocity and at 523 K. The molar ratio of CFC/H_2 or HCFC/H_2 was in the range 0.2–5.0 and feed partial pressures of CFC, HCFC and H_2 were between 120 and 640 Torr. The flow rates of CFC, HCFC, H_2 and Ar (as an inert gas) were controlled by Bronhorst Hi-Tec digital mass flow controllers. The reaction mixture outflowing from the reactor was analyzed by an on-line gas chromatograph using a PoraPLOT Q capillar column (30 m × 0.032 mm ID) and equipped with a FID detector.

3. Results and discussion

Table 1 shows some characterization data for the samples S_1, S_2 and S_3. Their chemical composition, determined by X-ray fluorescence, agrees with the elemental composition for the sample preparation.

Table 1
Characterization of the samples.

Sample	Chemical composition	BET area (m^2 g^{-1})	XRD phases[a]	Cell parameter (Å)
S_1	$KMg_{0.99}F_{2.98}$	41.1	P	3.9789 ± 0.0006
S_2	$KMg_{0.978}Pd_{0.021}F_{3.01}$	53.5	P	4.0007 ± 0.0001
S_3	$KMg_{0.935}Pd_{0.068}F_{3.0}$	46.8	P	4.0020 ± 0.0001

[a] P: perovskite phase.

The XRD patterns of the S_1, S_2 and S_3 samples are shown in figure 1 and can be indexed in the cubic system, spatial group Pm3m. The cell parameters were calculated collecting the data with an angular step of 0.05° at 5 s per step with silicon as an internal standard and using FULLPROF software [44]. The results, reported in table 1, show that there is an increase in the cell parameter of the samples higher than 0.002 nm when Pd^{2+} is incorporated in the perovskite-like structure due to its higher radius (0.086 nm) with respect to the Mg^{2+} (0.072 nm). There is also a correlation between the cell parameter and the palladium content of the perovskite. The incorporation of palladium in the perovskite structure is also confirmed by XRD spectra which did not show any line of a PdO phase (see figure 1 (b) and (c)). In contrast, when the pure $KMgF_3$ is impregnated with palladium in a similar amount as for the S_3 sample (hereafter called sample S_4) the XRD lines characteristic of the PdO phase are detected after calcination (see figure 1(d)).

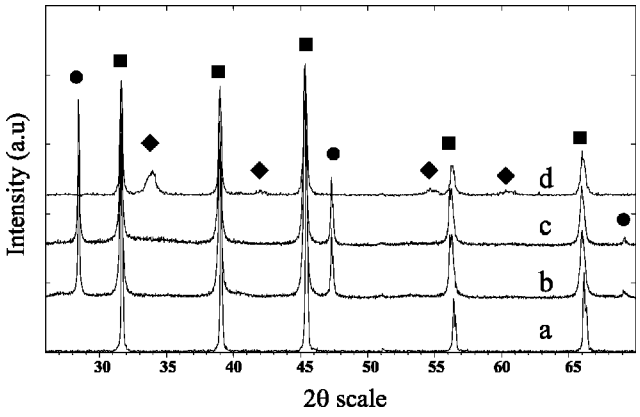

Figure 1. XRD for S_1 (a), S_2 (b), S_3 (c) and S_4 (d) samples. (•) Si, (■) perovskite and (⧫) PdO phases.

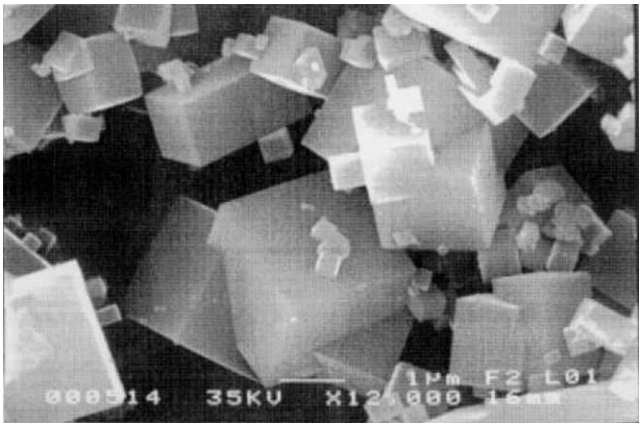

Figure 2. SEM micrograph of the sample S_1: $KMgF_3$ (magnification 12000×, reduced to 80% of original size).

The specific surface areas of the samples are in the range 41–53 $m^2\,g^{-1}$ (see table 1). The surface areas are slightly higher for the Pd samples. The SEM of the obtained solid exhibits cubic particles (see figure 2) where the average length of corners ranges from 0.2 to 5 μm. Samples with palladium show a lower length of corners. This observation agrees with the values of specific surface area.

In order to study the thermal stability of the synthesized samples, TG-DTA analyses in an argon-flowing atmosphere were performed. Neither phase transformations nor mass losses were observed between 393 and 873 K. This indicates that the samples are not hydrated and are stable, in agreement with the data reported in the literature [40,41]. This fact is confirmed by FT-IR spectra of samples showing no absorption bands of water at around 3450 and 1650 cm^{-1}. This is the first time that the preparation of a $KMg_{1-x}Pd_xF_3$ perovskite-like compound containing noble metal is reported.

After reduction, all the samples show XRD lines characteristic of Pd and $KMgF_3$ phases. Besides, S_{2R} and S_{3R} catalysts also show the presence of MgF_2 and KF phases in trace amounts. These phases are segregated from the bulk perovskite-like structure during the reduction process concurrently with Pd phase formation. The palladium particle sizes, calculated by using the Scherrer equation, were 4 nm for catalysts S_{2R} and S_{3R} and 10 nm for catalyst S_{4R}.

The catalytic results for the reaction of CCl_2F_2 and $CHClF_2$ with hydrogen, at steady state conditions, are shown in table 2. The main organic compounds obtained for the hydroconversion reaction of CCl_2F_2 were $CHClF_2$, CH_2F_2 and CH_4. These compounds represent more than 99% of the products. It is important to mention the high selectivity to $CHClF_2$ (between 44 and 75%) obtained from these catalysts, in contrast with the data reported previously using other Pd-based catalysts [12,13,16,18], where $CHClF_2$

Table 2
Catalytic properties for the hydrogenation of CCl_2F_2 and $CHClF_2$ over $Pd/KMgF_3$ and $KMg_{1-x}Pd_xF_3$ catalysts.[a]

Catalyst	Hydroconversion of CCl_2F_2						Hydroconversion of $CHClF_2$					
	R[b]	Conv. (%)	Product selectivities (mol%)				R[b]	Conv. (%)	Product selectivities (mol%)			
			CH_4	CH_2F_2	$CHClF_2$	Others[c]			CH_4	CH_2F_2	CH_3F	Others[d]
S_{2R}	22	1	3	22	75	–	27	1.2	20	80	–	–
S_{3R}	195	9	8	35	57	–	92	4.2	9	91	–	–
S_{4R}	283	13	20	35	44	1	37	1.5	26	28	43	3

[a] Reaction temperature 523 K, $H_2/CCl_2F_2 = 1$.
[b] Reaction rate expressed in (mol min^{-1} g^{-1}) × 10^7.
[c] CH_3Cl, CH_3F.
[d] CHF_3, C_2H_6, C_2H_4 and CH_3Cl.

Table 3
Influence of conversion on selectivity for the hydrogenation of CCl_2F_2 over $Pd/KMgF_3$ and $KMg_{1-x}Pd_xF_3$ catalysts.[a]

Catalyst	Conversion	Product selectivities (mol%)			
	(%)	CH_4	CH_2F_2	$CHClF_2$	Others[a]
S_{2R}	1	3	22	75	–
	6	4	19	77	–
	17	6	22	72	–
S_{3R}	9	8	35	57	–
	27	7	39	54	–
	53	9	40	51	–
S_{4R}	13	20	35	44	1
	23	22	45	33	–
	48	18	60	21	1

[a] Reaction temperature 523 K, $H_2/CCl_2F_2 = 1$.
[b] CH_3Cl, CH_3F.

is obtained as a minor product (<15%). The S_{2R} catalyst, which has the lowest Pd content in the perovskite-like structure and also the lowest activity, shows the highest selectivity to $CHClF_2$ (around 75%). The S_{4R} catalyst shows the highest reaction rate for the hydroconversion of CCl_2F_2 and also the lowest selectivity to $CHClF_2$ (around 44%).

It has been reported that the addition of high amount of HCl to the reaction feed ($H_2/HCl = 1$) using Pd/C catalyst causes an important increase in the selectivity to $CHClF_2$ (around 40%) for a 13% of conversion [19]. However, this Pd/C catalyst only shows a selectivity to $CHClF_2$ around 20% without the addition of HCl. The formation of $CHClF_2$ during the hydroconversion of CCl_2F_2 is explained by the reaction between CF_2 and chlorine species both adsorbed on the surface of the catalyst. Therefore, the S_{4R} catalyst, which shows the highest conversion and consequently the highest HCl amount (obtained as a product during the hydroconversion reaction), should have the highest selectivity to $CHClF_2$. However, the S_{2R} catalyst, with the less conversion, has the highest selectivity to $CHClF_2$ (around 75%). The influence of conversion level on selectivity was examined by modifying the spatial velocity. As show in table 3 the selectivity to $CHClF_2$ was maintained for S_{2R} and S_{3R} catalysts at conversion levels up to 15 and 50%, respectively. However, for the S_{4R} catalyst there is an increase in the selectivity to CH_2F_2 (mainly at the expense of $CHClF_2$) at high conversion level (around 50%).

Table 2 also shows the catalytic results for the hydroconversion of $CHClF_2$ using S_{2R}, S_{3R} and S_{4R} catalysts. The main product is CH_2F_2 for S_{2R} and S_{3R} catalysts (between 80 and 90%), while for S_{4R} the main product is CH_3F. Besides, the S_{3R} catalyst shows both highest reaction rate and selectivity to CH_2F_2 (around 90%). Therefore, S_{2R} and S_{3R} catalysts differ in catalytic behaviour with respect to S_{4R} during the hydroconversion of CCl_2F_2 and $CHClF_2$ (mainly). The Pd surface area, determined by hydrogen chemisorption for S_{2R}, S_{3R} and S_{4R} catalysts, were 0.2, 0.6 and 1.6 $m^2\,g^{-1}$, respectively (assuming $H_{irr}/Pd = 1$). This fact cannot explain the different catalytic behaviour of these catalysts. It seems that the interaction between the Pd metal particle and the support ($KMgF_3$) could play an important role in the hydrogenation reaction of CCl_2F_2 and $CHClF_2$ using our catalyst.

It is well known that the gas phase hydrogenation of CCl_2F_2 and $CHClF_2$ over supported Pd catalysts is greatly affected by the nature of the support [12,18]. Therefore, it could be speculated that the very different behaviour of Pd arises from the anchoring of Pd in the perovskite-like structure ($KMg_{1-x}Pd_xF_3$) than when supported on $KMgF_3$ or in other supports [12,13,16,18].

Coq *et al.* [12,18] reported that using palladium catalysts CH_4 and CH_2F_2 are the main products from hydroconversion of CCl_2F_2 on Pd/ZrF_4,TiF_4, AlF_3 and that CH_4 and CH_3F are the main products from hydroconversion of $CHClF_2$ on Pd/AlF_3. They suggest that the preferred reactions are those which allow the removal of two halogen atoms per sojourn on the surface of the catalysts. In contrast, when using $KMg_{1-x}Pd_xF_3$ catalysts (S_{2R} and S_{3R}), the most favourable reaction, for the hydroconversion of CCl_2F_2 and $CHClF_2$ is that which allows the removal of one chlorine atom during one sojourn on the surface of the catalysts, obtaining higher selectivities to $CHClF_2$ and CH_2F_2, respectively. In contrast, for S_{4R} catalyst the main obtained product for $CHClF_2$ hydrodechlorination is CH_3F.

Therefore, it seems that there is also a different behaviour between S_{2R}, S_{3R} and S_{4R} catalysts during the hydroconversion reaction of $CHClF_2$. This fact could be explained taking into account a different metal–support interaction for S_{2R} and S_{3R} with respect to S_{4R} which could modify favourably the electronic state of the metal particles. This could be related with the different way of catalysts preparation.

It is important to mention that after the reduction of S_2 and S_3 samples (which have perorvskite-like structure $KMg_{1-x}Pd_xF_3$) the phases detected by XRD are Pd and $KMgF_3$ (mainly), and also traces of KF and MgF_2 for the corresponding S_{2R} and S_{3R} catalysts. The latter phases are segregated from the structure of $KMg_{1-x}Pd_xF_3$ when the Pd^{2+} is reduced to Pd^0. Besides, only Pd and $KMgF_3$ phases are detected for catalyst S_{4R}.

Figure 3 (a) and (b) shows the effect of the H_2/HCFC ratio during the hydroconversion reaction of $CHClF_2$ for catalysts S_{4R} and S_{3R}, respectively. The catalytic behaviour of the two catalysts is very different, as observed. The main product is CH_2F_2 (around 85–91%) for catalyst S_{3R} with a slight decrease when the H_2/HCFC ratio increases, while the main product for catalyst S_{4R} is CH_3F followed by CH_2F_2 and CH_4 with values of around 40, 28 and 26%, respectively. At low H_2/HCFC ratio the CH_3F increases at the expense of the other products for the S_{4R} catalyst.

Figure 4 shows the conversion and products selectivity for catalyst S_{3R} as function of time on stream. Conversion and selectivity remain practically constant. Therefore, this catalyst does not show deactivation during 5 days time-run which leads us to assume that it has good stability to the HCl and HF action produced during the reaction.

After catalytic reaction and at steady state conditions, the diffraction patterns of the used S_{3R} catalyst shows a more

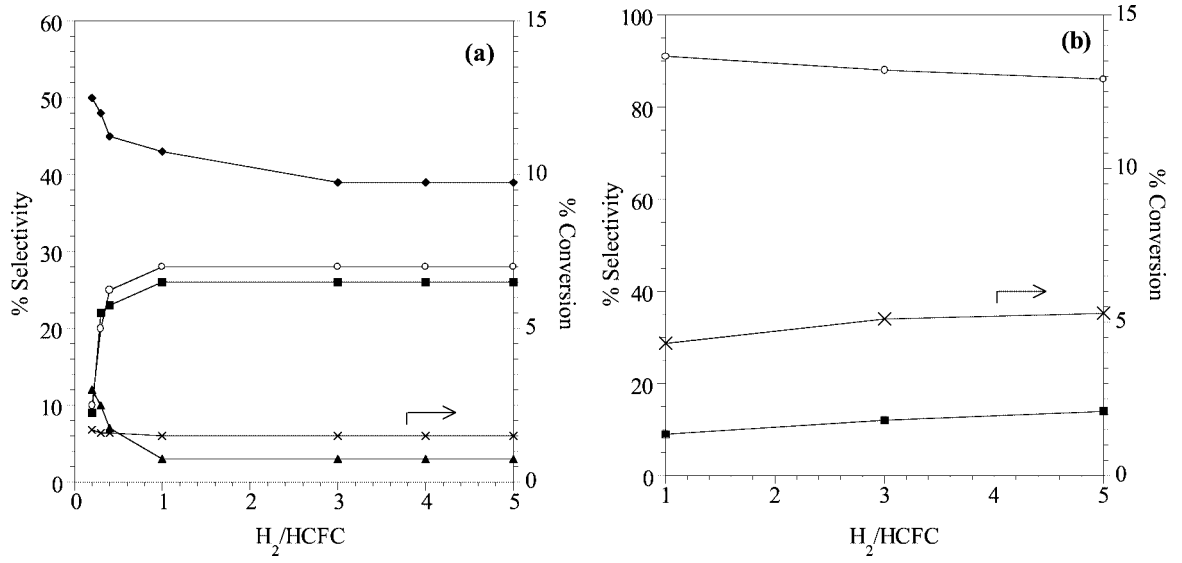

Figure 3. Conversion and product selectivities for the hydroconversion of $CHClF_2$ over (a) S_{4R} and (b) S_{3R} as a function of feed composition. Temperature of reaction 523 K. (○) CH_2F_2, (■) CH_4, (♦) CH_3F, (▲) other products and (×) conversion.

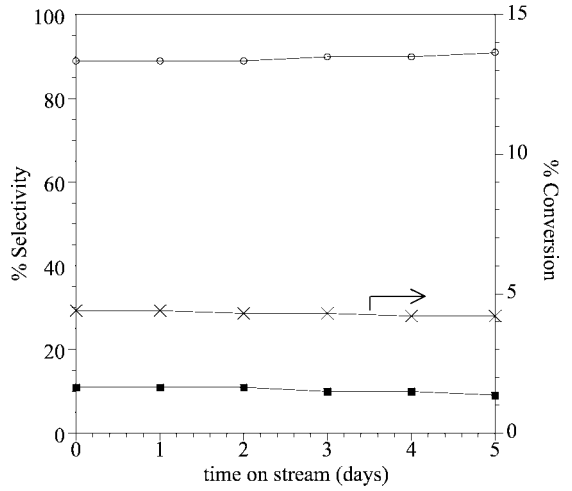

Figure 4. Conversion and product selectivities for the hydroconversion of $CHClF_2$ *vs.* time on reaction for catalyst S_{3R}. Temperature of reaction 523 K. $H_2/CHClF_2 = 1$. (○) CH_2F_2, (■) CH_4, (♦) CH_3F and (×) conversion.

crystalline MgF_2 phase and the appearance of one new and crystalline KCl phase. The KCl phase can be produced by the reaction of the KF phase, detected after the reduction of the perovskite-like structure, with the HCl released during the hydroconversion reaction. Besides, used S_{3R} catalyst also shows the presence of a small amount of a new PdC_x phase (figure 5(a)).

The appearance of PdC_x is due to the reaction of carbonaceous species formed during the reaction with the palladium [25,26,45–47]. The formation of this PdC_x phase could be related to the lower Pd particle size [26], and its higher interaction with the support for catalyst S_{2R} and S_{3R}.

It is important to mention that catalyst S_{4R} mainly shows, after catalytic reaction, two phases: Pd and $KMgF_3$. Also, traces of KCl are observed for the S_{4R} used catalyst (figure 5(b)) which can be due to the reaction of HCl produced during the reaction with some KF amorphous phase obtained

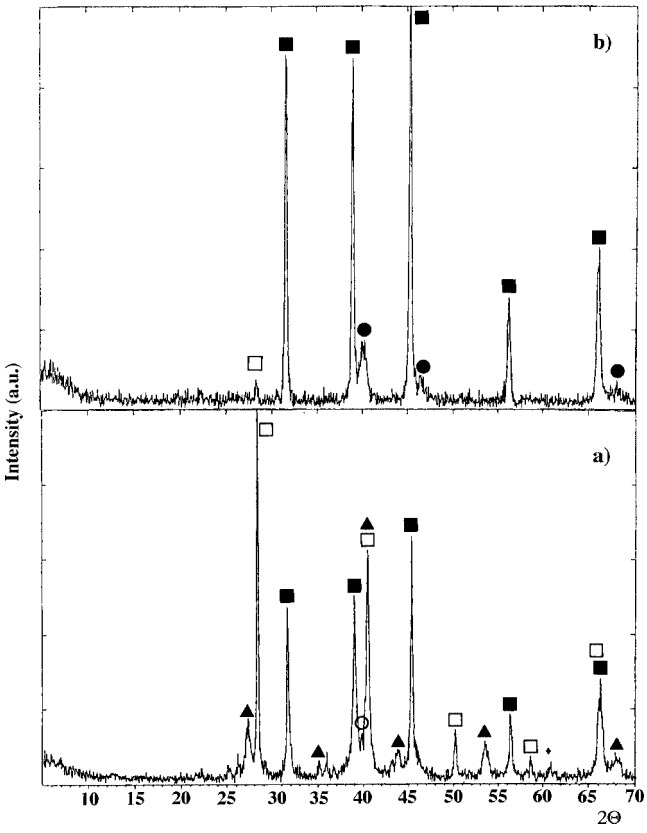

Figure 5. XRD for used catalysts: (a) S_{3R} and (b) S_{4R}. (■) Perovskite, (●) Pd, (□) KCl, (▲) MgF_2 and (○) PdC_x phases.

during the synthesis of $KMgF_3$ sample but undetected previously by XRD.

No PdC_x phase was detected for this catalyst, probably due to the higher particle size of the palladium and its lower interaction with the support. It seems that this palladium carbide phase also has an important role in the selectivity [46].

Therefore, complex fluorides with perovskite-like structure are very promising materials to obtain new Pd catalysts with interesting properties for the selective removal of only one chlorine atom from CCl_2F_2 and $CHClF_2$ molecules. Moreover, due to the very special properties of Pd in such an environment, unexpected catalytic properties of Pd might be found in other selective hydrogenation reactions.

Acknowledgement

The authors are grateful for the financial support of the Ministerio de Eduación y Cultura (AMB98-0545, HF1999-0144), and Kal y Sol Iberia S.A. AM acknowledges to Generalitat de Catalunya (BE99) for a grant in Montpellier.

References

[1] F.S. Rowland and M.J. Molina, Nature 249 (1974) 810.
[2] W. Brune, Nature 379 (1996) 486.
[3] Executive Summary of the Scientific Assessment of Ozone Depletion (1991).
[4] Programme for Alternative Fluorocarbon Toxicity Testing, Report of PAFT-V: HFC-32 (September 1992).
[5] United Nations Environmental Programme, Report of the Ad Hoc Technical Advisory Committee on ODS Destruction Technologies (May 1992).
[6] G.L. Li, G.I. Tatsumi, M.O. Yoshihiko and T. Yusaku, Appl. Catal. B 9 (1996) 239.
[7] E. Kemnitz, A. Kohne and E. Lieske, J. Fluorine Chem. 81 (1997) 197.
[8] X. Fu, W.A. Zellner, Q. Yang and M.A. Anderson, J. Catal. 168 (1997) 482.
[9] C.F. Ng, S. Shan and S.Y. Lai, Appl. Catal. A 16 (1998) 209.
[10] C. Gervasutti, L. Marangoni and W. Parra, J. Fluorine Chem. 19 (1981) 1.
[11] L.E. Manzer and V.N. Malikarjuna Rao, Adv. Catal. 39 (1992) 329.
[12] B. Coq, J.M. Cognion, F. Figuéras and D. Tournigand, J. Catal. 141 (1993) 21.
[13] A. Wiersma, E.J.A.X. van de Sandt, M.A. Hollander, H. van Bekkum, M. Makkee and J.A. Moulijn, J. Catal. 177 (1998) 29.
[14] B.S. Ahn, S.C. Lee, D.J. Moon and B.G. Lee, J. Mol. Catal. 106 (1996) 83.
[15] S. Deshmukh and J.L. d'Itri, Catal. Today 40 (1998) 377.
[16] A. Malinowski, W. Juszcyk, M. Bonarowska, J. Pielaszek and Z. Karpinski, J. Catal. 177 (1998) 153.
[17] A. Malinowski, W. Juszczyk, J. Pielaszek, M. Bonarowska, M. Wojciechowska and Z. Karpinski, Chem. Commun. (1999) 685.
[18] B. Coq, F. Figuéras, S. Hub and D. Tournigant, J. Phys. Chem. 99 (1995) 11159.
[19] E.J.A.X. van de Sandt, A.W. Wiersma, M. Makke, H. van Bekkum and J.A. Moulijn, J. Recl. Trav. Chim. Pays-Bas 115 (1996) 505.
[20] H. Kim, H.S. Kim, B.G. Lee, H. Lee and S. Kim, Chem. Commun. (1995) 2383.
[21] I. Dogson, Stud. Surf. Sci. Catal. 78 (1993) 1.
[22] Z. Karpinski, D. Early and J.L. d'Itri, J. Catal. 164 (1996) 378.
[23] W. Juszczyk, A. Malinowski and Z. Karpinski, Appl. Catal. A 166 (1998) 311.
[24] F. Ribeiro, C.A. Gerken and G.A. Somorjai, Catal. Lett. 45 (1997) 149.
[25] E.J.A.X. van de Sandt, A. Wiersma, M. Makkee, H. van Bekkum and J.A. Moulijn, Catal. Today 35 (1997) 163.
[26] A. Morato, C. Alonso, F. Medina, Y. Cesteros, P. Salagre, J.E. Sueiras, D. Tichit and B. Coq, Appl. Catal. B 33 (2001) 167.
[27] G. Rupprechter and G. Somorjai, Catal. Lett. 48 (1997) 17.
[28] G.J. Moore and J. O'Kelly, Eur. Patent Application 508660 (1992), to ICI.
[29] J.P. Schoebrechts and V. Wilmet, US Patent 5561096 (1994), to Solvay.
[30] Y. Zhao, J. Solid State Chem. 141 (1998) 121.
[31] M. Eibschutz and H.J. Guggenheim, Solid State Commun. 6 (1968) 737.
[32] M. Eibschutz, Phys. Lett. A 29 (1969) 409.
[33] D.K. Sardar, W.A. Sibley and R. Aicala, J. Luminesc. 27 (1982) 401.
[34] A.R. West, *Solid State Chemistry and its Applications* (Wiley, New York, 1984) p. 338.
[35] R.A. Heaton and C.L. Chun, Phys. Rev. B 25 (1982) 3538.
[36] V.K. Domar, A.V. Gektin, N.P. Ivanow, Y.A. Nesterenko and N.V. Shiran, J. Cryst. Growth 166 (1996) 419.
[37] A. Ratuszna, M. Rousseau and P. Daniel, Powder Diff. 12 (1997) 70.
[38] Al. Darabont, C. Neamtu, S.I. Farcas and Gh. Borodi, J. Cryst. Growth 169 (1996) 89.
[39] M. Martini, F. Meinardi and A. Scacco, Chem. Phys. Lett. 293 (1998) 43.
[40] C. Zhao, S. Feng, R. Xu, C. Shi and N. Ni, Chem. Commun. (1997) 945.
[41] C. Zhao, S. Feng, Z. Chao, C. Shi, R. Xu and J. Ni, Chem. Commun. (1996) 1641.
[42] W.P. Hsu, Q. Zhong and E. Matijevic, J. Colloid Interface Sci. 181 (1996) 142.
[43] J.E. Benson, H.S. Hwany and M. Boudart, J. Catal. 30 (1973) 146.
[44] R. Carvajal Jr., FULLPROF: A program for Rietveld refinement and pattern matching analysis, in: *Collected Abstracts of Powder Diffraction Meeting*, Toulouse, France, 1990, p. 127.
[45] S.B. Ziemecki, G.A. Jones, D.G. Swartzfager and R.L. Harlow, J. Am. Chem. Soc. 107 (1985) 4547.
[46] B.S. Ahn, S.G. Jeon, H. Lee, K.Y. Park and Y.G. Shul, Appl. Catal. A 193 (2000) 87.
[47] W. Juszczyk, A. Malinowski and Z. Karpinski, Appl. Catal. A 166 (1998) 311.